arXiv:1611.04343v1 [gr-qc] 14 Nov 2016

Gravitational Lensing by Multi-Polytropic Static Wormholes

S.N. Sajadi*, N. Riazi†
Department of Physics, Shahid Beheshti University, G.C., Evin, Tehran 19839, Iran

November 15, 2016

Abstract

We obtain multi-polytropic static solutions in the framework of **GR** gravity. The resulting metric is asymptotically Minkowskian, and locally that of a wormhole. We also examine gravitational lensing by the wormhole, and calculate the deflection angle for weak and strong field limits. We investigate microlensing for unbounded wormhole in weak field limit and obtain corresponding light curves for both galactic and extragalactic situations. We discuss the multi-polytropic equation of state for the energy-momentum tensor which supports this geometry and finally, we check for the weak energy condition.

1 Introduction

In classical general relativity the Einstein field equations admit a simple and interesting class of static solutions describing tunnels in spacetime, connecting either two remote regions of our Universe or even different universes. These geometrical objects are called wormholes. Historically, the concept of a wormhole was suggested by Ludwig Flamm by looking at the simplest solution of Einsteins field equation (i.e. the Schwarzschild solution), in 1916, shortly after the publication of the Einstein field equations, by means of the now standard embedding diagram. By using of time symmetry of the solution, Flamm realized that Einstein equations allowed a second solution, now known as a white hole[1]. In 1935, a similar construction was later explored by Einstein and Rosen in a paper whose actual purpose was to explain fundamental particles, such as electrons, in terms of spacetime tunnels threaded by electric lines of force [2], the so-called Einstein-Rosen bridge [3]. The concept of traversable wormhole was suggested by Morris and Thorne with the idea of using a wormhole for interstellar travel or even time travel [4] . Wormhole physics is a specific example of adopting the reverse philosophy of solving the Einstein field equation, by first constructing the spacetime metric, then deducing the stress-energy tensor components. Thus, it was found that these traversable wormholes possess a stress-energy tensor that violates the null energy condition. In fact, they violate all the known pointwise energy conditions and averaged energy conditions, which are fundamental to the singularity theorems and theorems of classical black hole thermodynamics. In the opposite direction, if the exotic matter is removed from the wormholes throat, then the wormhole could decay into a black hole. It has been shown that the wormhole region that requires exotic matter can be made arbitrary small by introducing a special shape function [5]. It is remarkable that wormhole configurations may be constructed without

*Electronic address: naseh.sajadi@gmail.com
†Electronic address: n_riazi@sbu.ac.ir

needing any form of exotic matter sources in the framework of alternative theories of gravity, such as $f(R)$ gravity, Einstein-Gauss-Bonnet theory, Lovelock models, Brans-Dicke theory, among others[6, 7, 8, 9, 10, 11, 12, 13]. In spite of enthusiastic theoretical investigations, studies searching for observational evidence of the existence of wormholes are scarce. Only a few attempts have been made to show the existence or nonexistence of wormholes in our universe [14, 15, 16, 17]. A possible observational method that has been proposed to detect or exclude the existence of wormholes is the application of optical gravitational lensing, since the light ray propagation is sensitive to a local spacetime geometry.
From an observational point of view, lensing provided the first experimental verification of GR through observations of starlight bending around the Sun during an eclipse in 1919 and continues to be a major source of insight into gravitation. Gravitational lensing is an important window to look for signatures of astrophysical objects such as black holes and dark matter halos. Early works focused on the lensing phenomenon in the weak field, but weak field results can not distinguish between different solutions that are asymptotically flat. For this reason, one must check the strong limit of gravitational lensing. What one needs for this purpose is a method of calculation. In fact, it is difficult to investigate the relations between the deflection angle and the properties of gravitational source because the deflection angle of light passing close to a compact and massive source is known in integral forms. The difficulty is that, light deflection diverges at the photon sphere (corresponding to unstable orbits that photon approaches close enough to the object such that it can loop once, twice, or any amount of times before reaching the observer) [18]. Progress in this direction was initiated by Fritelli, Kling and Newman [19], and by Virbhadra and Ellis [20]. When the light goes very close to a heavy compact body like a black hole, it will provide more information about the nature of the gravitational source's surrounding.

Cramer et al.[14] and Torres et al.[15] have recently studied the microlensing effects of a negative mass wormhole on the light from a background point-like source. These authors have shown that the typical light curves expected from microlensing events produced by wormholes should be very different from the light curves in positive mass microlensing of point sources. Also, these authors showed that the effective gravitational repulsion of light rays creates two bursts, which are individually asymmetric under time reversal, although mirror images of each other. Recently, Anchordoqui et al. [21] searched in existent gamma-ray burst databases for signatures of wormhole microlensing. Although they detected some interesting candidates, no conclusive results were claimed [21, 22].

In the present work, we introduce a new exact wormhole metric which is supported by a multi-polytropic matter source. Polytropic equations of state are important in a variety of astrophysical applications. Traditionally, the polytropic equation of state has been used to describe a completely degenerate gas in Newtonian theory and special relativity, an isothermal ideal gas and a completely convective star [23]-[31]. There is still a debate over the structure of a star as to its composition in terms of nuclear matter, or quark matter, or a hybrid mix of both distributions. Our motivation for considering a multi-polytropic EoS which is softer at low densities and stiffer at high densities may be appropriate for describing a hybrid object. After all, a more general EoS provides a better fit, thereby increasing the freedom to describe naturally occurring astronomical objects [32]. In Section. 2, the general wormhole formalism is presented. In section 3 the formalism of gravitational lensing and microlensing is reviewed. In section 4, we solve the Einstein equations for multi-polytropic, spherical wormhole and then calculate the lensing deflection angle numerically. In section 5, we investigate the corresponding energy-momentum tensor and discuss the energy condition. The last section is devoted to conclusions and closing remarks.

2 Wormhole Formalism

In the pioneering work of Morris and Thorne, they described a general class of solutions of Einstein equations representing wormholes [4]. The conditions that they imposed in order to obtain the general form of the metric tensor included:
1. The metric must be spherically symmetric and static (independent of time).
2. The solution must have a throat joining two asymptotically flat regions of spacetime.
3. The metric must satisfy Einstein equations in every point of spacetime.
4. The geometry will not have event horizons nor singularities.
Under these conditions, the general form for the metric tensor is:

$$ds^2 = -e^{2\Phi(r)}dt^2 + \frac{dr^2}{1-\frac{b(r)}{r}} + r^2(d\theta^2 + r^2\sin^2(\theta)d\phi^2) \tag{1}$$

where $\Phi(r)$ and $b(r)$ are arbitrary functions of the radial coordinate r. $\Phi(r)$ is called the redshift function, for it is related to the gravitational redshift, and $b(r)$ is known as the shape function, because as can be shown by embedding diagrams, it determines the shape of the wormhole. The coordinate r is non-monotonic in that it decreases from $+\infty$ to a minimum value r_0, representing the location of the throat of the wormhole, where $b(r_0) = r_0$, and then it increases from r_0 to $+\infty$. The proper circumference of a circle of fixed r centered at the wormhole is given by $2\pi r$, with the minimum value $2\pi r_0$ at the throat. Although the metric coefficient g_{rr} becomes divergent at the throat, which is signalled by the coordinate singularity, the proper radial distance

$$l(r) = \pm\int_{r_0}^{r} \frac{dr}{(1-\frac{b(r)}{r})^{\frac{1}{2}}} \tag{2}$$

should be finite. Note that as $0 \leq 1 - b(r)/r \leq 1$, the proper distance is greater than or equal to the coordinate distance, i.e., $|l(r)| \geq r - r_0$. The metric 1 may be written in terms of the proper radial distance as

$$ds^2 = -e^{2\Phi(l)}dt^2 + dl^2 + r^2(l)[d\theta^2 + \sin^2(\theta)d\phi^2]. \tag{3}$$

The proper distance decreases from $l = +\infty$, in the upper universe, to $l = 0$ at the throat, and then from zero to $-\infty$ in the lower universe. For the wormhole to be traversable, it must have no horizons, which implies that $g_{tt} = -\exp(2\Phi(r)) \neq 0$, so that $\Phi(r)$ must be finite everywhere. We can use embedding diagrams to represent a wormhole and extract some useful information for the choice of the shape function $b(r)$. Due to the spherically symmetric nature of the problem, one may consider an equatorial slice, $\theta = \frac{\pi}{2}$, without loss of generality. The respective line element, considering a fixed moment of time, $t = const$, is given by

$$ds^2 = \frac{dr^2}{1-\frac{b(r)}{r}} + r^2d\phi^2 \tag{4}$$

To visualize this slice, one embeds this metric into three-dimensional Euclidean space, in which the metric can be written in cylindrical coordinates, (r, ϕ, z), as

$$ds^2 = dz^2 + dr^2 + r^2d\phi^2 \tag{5}$$

Now, in the three-dimensional Euclidean space the embedded surface has equation $z = z(r)$, and thus the metric of the surface can be written as,

$$ds^2 = [1 + (\frac{dz}{dr})^2]dr^2 + r^2d\phi^2 \tag{6}$$

Comparing Eq. 6 with 4, we have the equation for the embedding surface, given by

$$\frac{dz}{dr} = \pm(\frac{r}{b(r)} - 1)^{-\frac{1}{2}} \tag{7}$$

To be a wormhole solution, the geometry must have a minimum radius, $r = b(r) = r_0$, denoted as the throat, at which the embedded surface is vertical, i.e., $\frac{dz}{dr} \longrightarrow \infty$. Far from the throat space is asymptotically flat, $\frac{dz}{dr} \to 0$ as $r \to \infty$. One also needs to impose that the throat flares out. Mathematically, this flaring-out condition entails that the inverse of the embedding function $r(z)$ must satisfy $\frac{d^2r}{dz^2} > 0$ at or near the throat r_0. Differentiating $\frac{dr}{dz} = \pm(\frac{r}{b(r)} - 1)^{\frac{1}{2}}$ with respect to z, we have

$$\frac{d^2r}{dz^2} = \frac{b - b'r}{2b^2} > 0 \tag{8}$$

At the throat, we verify that the shape function $b(r)$ satisfies the condition $b'(r_0) < 1$. This condition plays a fundamental role in the analysis of the violation of the energy conditions[4, 33, 34]. To gain some insight into the matter threading the wormhole, Morris and Thorne defined the dimensionless function

$$\zeta = \frac{\bar{P} - \rho}{\rho} = \frac{P_r + 2P_t - 3\rho}{3\rho}. \tag{9}$$

The wormhole material is exotic, i.e., $\zeta > 0$, and nonexotic if $\zeta < 0$. ζ is thus called the exoticity parameter[4, 6, 35].

3 Gravitational Lensing and Microlensing by the Wormhole

Gravitational lensing occurs when a gravitating mass distorts a spacetime and the geodesic of anything passing through it. The paths followed by electromagnetic radiation from a star, galaxy, or other source are bent as well. This can be seen directly from equations of motion for photons. To show the effect of a gravitating mass on the path of light, we consider a general spherically symmetric and static line element:

$$ds^2 = -A(r)dt^2 + B(r)dr^2 + C(r)(d\theta^2 + \sin^2(\theta)d\phi^2). \tag{10}$$

Photons follow the equations of motion for null geodesics:

$$\frac{d^2x^\mu}{d\lambda^2} + \Gamma^\mu_{\alpha\beta}\frac{dx^\alpha}{d\lambda}\frac{dx^\beta}{d\lambda} = 0 \tag{11}$$

where λ is the affine parameter and $\frac{dx^\mu}{d\lambda}$ represents the four-velocity of the photons. In a spherically symmetric spacetime, the lens, observer, and source can all be placed on a single plane with a constant value of $\theta = \frac{\pi}{2}$, so $\dot{\theta} = 0$. Without loss of generality the metric reduces to:

$$ds^2 = -A(r)dt^2 + B(r)dr^2 + C(r)d\phi^2. \tag{12}$$

Since the metric is independent of t and ϕ, there are two conserved quantities:

$$A(r)\dot{t} = E \qquad , \qquad C(r)\dot{\phi} = J. \tag{13}$$

For the metric 10, the geodesic equation becomes:

$$-\frac{1}{u^2} + \frac{A(r)B(r)}{J^2}(\frac{dr}{d\lambda})^2 + \frac{A(r)}{C(r)} = 0 \quad , \quad where \;\; u = \frac{J}{E} = \sqrt{\frac{C(r_m)}{A(r_m)}}. \tag{14}$$

A light ray travels from left to right, and we want to know how much ϕ changes as the light ray moves from the left side to the right side. The light ray travels from large r to a minimum r_m and then out to large r again. Since both the source and the observer are located very far from the lens and there is negligible deflection far away from the lens, we can treat both as located at $r = \infty$. To calculate the change in ϕ with r over the light rays trajectory, we perform the integral:

$$\alpha(r_m) = 2\int_{r_m}^{\infty} \frac{d\phi}{dr} dr - \pi = 2\int_{r_m}^{\infty} \frac{\dot{\phi}}{\dot{r}} dr - \pi. \tag{15}$$

where $\alpha(r_m) = \phi(+\infty) - \phi(-\infty)$ is the deflection of light due to a mass as a function of its point of closest approach. This integral sums the deflection at each value of r from r_m to ∞. This can be interpreted as the deflection that occurs during light's trip from r_m to the observer. The integral is multiplied by two to take into account the deflection that takes place during its trip from the source to r_m. By using Eqs. 13 and 14, we obtain:

$$\alpha(r_m) = \int_{r_m}^{\infty} \frac{2\sqrt{B(r)}dr}{\sqrt{C(r)}\sqrt{\frac{C(r)A(r_m)}{C(r_m)A(r)} - 1}} - \pi. \tag{16}$$

Because this integration can not be performed exactly for most metrics, usually it is approximated the weak and strong cases[19, 36]. By applying the above general result and using the limit $\frac{M}{r_m} << 1$ (weak field limit) to the Schwarzschild metric one obtains the following result

$$\alpha(r_m) = \frac{4M}{r_m} \tag{17}$$

which is used for almost all astrophysical considerations of lensing. In a strong field limit people commonly use Bozza$'$s method to calculate lensing effect of objects[19]. The method of Bozza is to expand the integral in Eq. 16 around the photon sphere to obtain a logarithmic expression for $\alpha(r_m)$. According to that procedure the deflection angle is obtained as follows

$$\alpha(\theta) = -\bar{a}\ln(\frac{\theta D_{OL}}{u_m} - 1) + \bar{b}, \tag{18}$$

where $\bar{a}$ and $\bar{b}$ are constants and u_m, D_{OL} are the impact parameter of the light and the distances from the observer to the lens, respectively [37]-[41]. The angle between the lens (wormhole) and the source β can then be written as

$$\beta = \frac{\xi}{D_L} - \frac{D_{LS}}{D_S}\alpha(r), \tag{19}$$

where D_L, D_S, D_{LS}, and ξ are the distances from the observer to the lens, from the observer to the source, and from the lens to the source, and the impact parameter of the light, respectively. If the source and lens are completely aligned along the line of sight, the image is expected to be circular (an Einstein ring). The Einstein radius R_E, which is defined as the radius of the circular image on the lens plane, is obtained from Equation with $\beta = 0$ as

$$R_E = \sqrt{\frac{4GM}{c^2}\frac{D_{LS}D_L}{D_S}}, \tag{20}$$

When both the lens and the source are moving with respect to each other, then images change their position and brightness. This effect is called microlensing. Angle β changes with time according to

$$\beta(t) = \sqrt{\beta_0^2 + (\frac{t - t_0}{t_E})^2}, \tag{21}$$

where β_0 is the impact parameter of the source trajectory and t_0 is the time of closest approach. t_E is the Einstein radius crossing time given by

$$t_E = \frac{R_E}{V_T}, \tag{22}$$

where V_T is the transverse velocity of the lens relative to the source and observer. Finally, the total amplification as a function of time ($t = t_0 \pm t_E$) is given by

$$A(t) = \frac{\beta(t)^2 \pm 2}{\beta(t)\sqrt{\beta(t)^2 \pm 4}}, \tag{23}$$

where the plus (minus) sign corresponds to the positive (negative) point mass case. When the source is extended, we must take into account the contributions coming from the different parts of it [42]. If the lens is extended and source is point like, then we can take into account the mass of lens enclosed to region with radius of impact parameter [43], or characterize an extended lens by its virial mass: the mass contained in a sphere with mean density equal to the virial density [44].
We will return to the lensing and microlensing problem in the next section, but before that, let us solve the Einstein equations for a wormhole metric with a multi-polytropic fluid as the source.

4 Einstein Field Equations and the Equation of State

We consider a static spherically symmetric space-time in the form of metric 1. The non-vanishing components of the Einstein tensor for our ansatz metric read

$$G_t^t = \frac{b'}{r^2}, \tag{24}$$

$$G_r^r = -\frac{b}{r^3} + 2(1 - \frac{b}{r})\frac{\Phi'}{r}, \tag{25}$$

and

$$G_\theta^\theta = G_\phi^\phi = (1 - \frac{b}{r})[\Phi'' + (\Phi')^2 - \frac{b'r - b}{2r(r - b)}\Phi' - \frac{b'r - b}{2r^2(r - b)} + \frac{\Phi'}{r}]. \tag{26}$$

We therefore need a diagonal energy-momentum tensor $T_\nu^\mu = diag(-\rho, P_r, P_t, P_t)$, with

$$\rho(r) = -\frac{1}{8\pi G}\frac{b'}{r^2}, \tag{27}$$

$$P_r = -\frac{1}{8\pi G}[\frac{b}{r^3} + 2(1 - \frac{b}{r})\frac{\Phi'}{r}], \tag{28}$$

and

$$P_t = \frac{1}{8\pi G}(1 - \frac{b}{r})[\Phi'' + (\Phi')^2 - \frac{b'r - b}{2r(r - b)}\Phi' - \frac{b'r - b}{2r^2(r - b)} + \frac{\Phi'}{r}]. \tag{29}$$

By taking derivative with respect to the radial coordinate r of Eq. 28, and after some algebra, we obtain the relativistic hydrostatic equation:

$$\frac{dP_r}{dr} = \frac{G(\rho + P_r)(M(r) + 4\pi r^3 P_r)}{r^2(1 - \frac{2GM(r)}{r})} - \frac{2(P_r - P_t)}{r} = (\rho + P_r)\Phi' - \frac{2}{r}(P_r - P_t) \tag{30}$$

where $M(r)$ is the gravitational mass inside a sphere of radius r

$$M(r) = \int_{r_0}^{r} 4\pi r^2 \rho dr \tag{31}$$

Here, we assume the multi-polytropic equation of state in the following form

$$P_r = A\rho + B\rho^{\frac{2n+2}{n+2}} \quad , \quad P_t = C\rho + D\rho^{\frac{2n+2}{n+2}} + E\rho^{\frac{3n+2}{n+2}}. \tag{32}$$

Although this equation of state is of a special type and lacks generality, it can still be a useful model for the following reasons. Even for nonrelativistic polytropic spheres which lead to the Lane-Emden equation, analytical solutions can be obtained only for few certain values of the polytropic index n ($n = 0, 1, 5$). For other values of the index (e.g. $n = 3$ etc.), only numerical or series solutions for small r can be found. Now, the relativistic case (i.e. the TOV equation) which is much more involved, it is impossible to obtain exact analytical solutions for an arbitrary equation of state [23, 27, 28]. This is why we have only numerical models for real astrophysical objects. Having an exact analytical solution should be interesting by its own. The cost, of course, is deviating from having a more realistic model.
By solving the hydrostatic equation and using the above equation of state, the red shift function and the shape function are obtained as follow:

$$\Phi(r) = -\frac{1}{2}(\frac{r_0}{r})^n \quad , \quad b(r) = r(\frac{r_0}{r})^n. \tag{33}$$

So, the metric turns out to be:

$$ds^2 = -e^{-(\frac{r_0}{r})^n}dt^2 + \frac{dr^2}{1 - (\frac{r_0}{r})^n} + r^2 d\theta^2 + r^2 \sin^2\theta d\phi^2. \tag{34}$$

Using the above metric and the Einstein equations, we obtain the energy-momentum tensor components:

$$\rho = -\frac{1}{8\pi G}T_t^t = -\frac{1}{8\pi G}[\frac{(\frac{r_0}{r})^n(n-1)}{r^2}], \tag{35}$$

$$P_r = \frac{1}{8\pi G}T_r^r = \frac{1}{8\pi G}[\frac{(n-1)(\frac{r_0}{r})^n}{r^2} - \frac{n}{r^2}(\frac{r_0}{r})^{2n}], \tag{36}$$

and

$$P_t = \frac{1}{8\pi G}T_\theta^\theta = \frac{1}{8\pi G}[\frac{-2n(n-1)}{4r^2}(\frac{r_0}{r})^n + \frac{n^2}{r^2}(\frac{r_0}{r})^{2n} - \frac{n^2}{4r^2}(\frac{r_0}{r})^{3n}]. \tag{37}$$

It can be seen that the spacetime is asymptotically flat if $n > 0$, For $n < 0$, We will have a closed space with less symmetries compared to the Einstein static universe. For the wormhole to be traversable $\Phi(r) = -\frac{1}{2}(\frac{r_0}{r})^n$ must be finite everywhere which again demands $n > 0$. The equation for the embedding surface is given by

$$\frac{dz}{dr} = \frac{1}{\sqrt{(\frac{r}{r_0})^n - 1}}. \tag{38}$$

At the throat, $r = r_0$, the embedding surface is vertical i.e: $\frac{dz}{dr} \longrightarrow \infty$. Far from the throat, the space is asymptotically flat, i.e as $r \longrightarrow \infty$, $\frac{dz}{dr} \longrightarrow 0$.
In order to check the flare-out condition at throat, we have

$$\frac{d^2r}{dz^2} = \frac{n}{2r}(\frac{r}{r_0})^n, \tag{39}$$

and since the form function satisfies the condition $b^{'}(r_0) < 1$, we should have

$$b^{'}(r_0) = (1-n)(\frac{r_0}{r})^n|_{r=r_0} = 1 - n < 1 \quad \longrightarrow \quad n > 0, \tag{40}$$

In which we have used Eq. 35. The gravitational mass $M(r)$ inside a sphere of radius r is

$$M(r) = \int_{r_0}^{r} 4\pi r^2 \rho dr = 4\pi r_0[-1 + (\frac{r_0}{r})^{n-1}] \tag{41}$$

which at the infinity ($r \longrightarrow \infty$) gives $M = -4\pi r_0$ if $n > 1$. In order to have positive energy density (positive mass), we must have $n < 1$, while, in the case of $n = 1$, we have massless wormhole. Therefore, in order to satisfy the above conditions (flare-out, asymptotically flatness, positive mass), we should have $0 < n < 1$.

4.1 The case $0 < n < 1$

In this interval, the mass function is positive throughout the spacetime, but unbounded as $r \to \infty$. In order to have a finite mass in this case, one has to put a thin-shell layer and glue the wormhole spacetime to a Schwarzschild external spacetime. As an example how this can be done, consider the following metric which continuously connect the wormhole metric to an outer Schwarzschild metric [45]:

$$ds^2 = -F(r)dt^2 + \frac{dr^2}{1 - \frac{2m}{r}} + r^2 d\Omega^2, \tag{42}$$

where

$$\frac{2m}{r_1} = (\frac{r_0}{r_1})^n \quad and \quad F(r) = \left[\frac{r - r_2}{r_1 - r_2}\right] e^{-(\frac{r_0}{r})^n} + \left[\frac{r - r_1}{r_2 - r_1}\right](1 - \frac{2m}{r}). \tag{43}$$

By using Eq. 17 for weak lensing and using Eq. 41, we have:

$$\alpha = \frac{4M}{r_m}. \tag{44}$$

according to this weak lensing approximation, as $r_m \to \infty$, the deflection angle goes to zero. The dashed part is excluded since $r < r_0$ in that region.

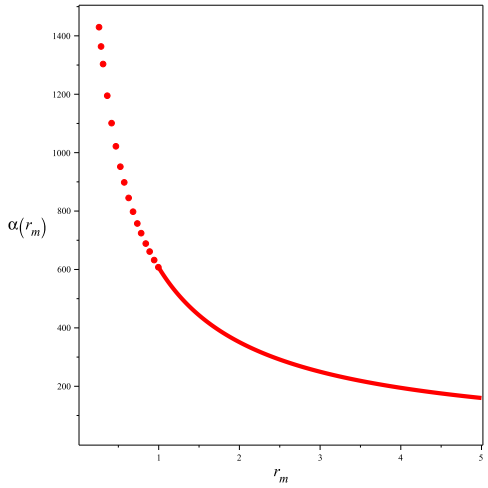

Figure 1: The behavior of α in terms of r_m at $r_0 = 1, M = 1000, n = \frac{1}{2}$. The dotted part should be excluded, since $r < r_0$ does not belong to the physical space time of the wormhole.

By using the wormhole metric and Eq. 16 for deflection angle, one obtains the following quadrature for lensing, if the metric 34 is used all over the space:

$$\alpha(r_m) = \int_{r_m}^{\infty} \frac{2dr}{r((1-(\frac{r_0}{r})^n)(\frac{r^2 e^{(\frac{r_0}{r})^n}}{r_m^2 e^{(\frac{r_0}{r_m})^n}} - 1))^{\frac{1}{2}}} - \pi, \tag{45}$$

where r_m is the coordinate of closest approach. If we rewrite the integral as follows

$$\alpha(r_m) = I(r_m) - \pi. \tag{46}$$

For a finite mass model, we use the technique described in section 4.1, and calculate $I(r_m)$ by splitting the integral into three parts $[r_0, r_1]$, $[r_1, r_2]$ and $[r_2, \infty]$. Each integral is evaluated by numerical methods. Results are plotted in Figure 2.

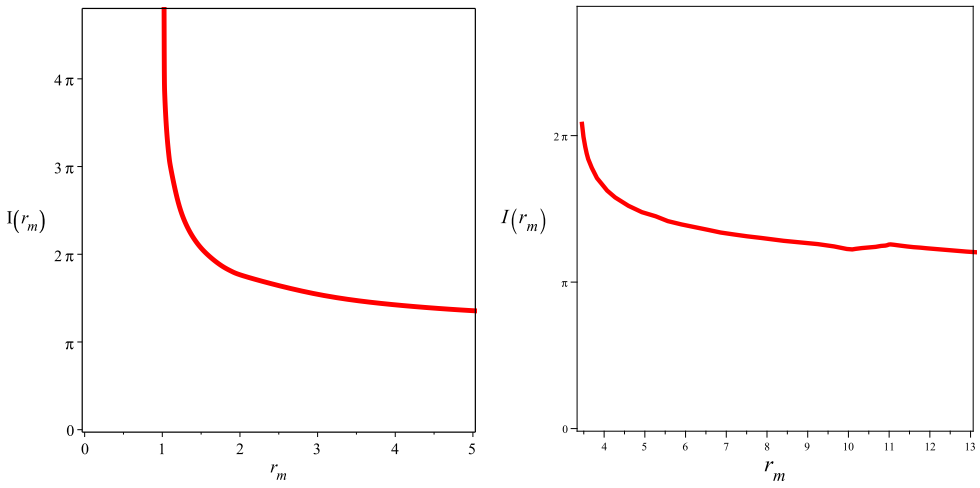

(a) (b)

Figure 2: The behavior of I in terms of r_m for $r_0 = 1$, $n = \frac{1}{2}$, if the metric 34 is used all over the space(left). The behavior of I in terms of r_m for $r_0 = 1, r_1 = 10, r_2 = 11, n = \frac{1}{2}$, and linearly-interpolated metric for the shell(right).

Full gravitational lensing (both weak and strong) can be read from Fig. 2a and Eq. 45. According to this figure, the behavior is similar to the Schwarzschild metric which has positive deflection angle, i.e. wormhole acts like convergent lens. Note that lensing calculations which have led to Fig. 2b are performed by assuming $r_0 = 1$, $r_1 = 10$ and $r_2 = 11$. Also, note that we have assumed the material medium to be transparent and non-refractive. Also the divergence occurs in the throat and corresponds to a photon sphere. As we get away from the photon sphere the $I(r_m)$ becomes smaller and eventually becomes π, That means at long distances the deflection angle goes to zero and this result is consistent with weak lensing.

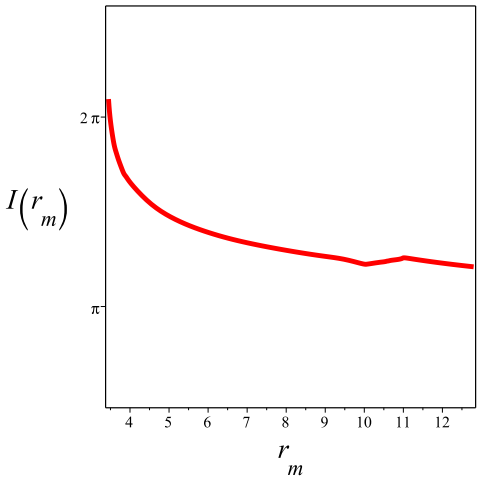

Figure 3: The behavior of I in terms of r_m for $r_0 = 1, r_1 = 10, r_2 = 11, n = \frac{1}{2}$, and quadratic-interpolation metric for the shell.

In order to ensure that the effect of the thin shell and the metric chosen for it are not critical

for the lensing, we have also considered a quadratic ansatz which satisfies the boundary conditions at r_1 and r_2:

$$ds^2 = -F(r)dt^2 + \frac{dr^2}{1-\frac{2m}{r}} + r^2 d\Omega^2, \tag{47}$$

where

$$F(r) = \left(\frac{r^2}{r_2(r_1-r_2)} + \frac{r_1 r}{r_2(r_2-r_1)} + 1\right) e^{-(\frac{r_0}{r})^n} + \left(\frac{r^2}{r_1(r_2-r_1)} + \frac{r_2 r}{r_1(r_1-r_2)} + 1\right)(1-\frac{2m}{r}) \tag{48}$$

Lensing is re-calculated with this metric for the intermediate shell (Figure 3). This figure shows that the difference with linear ansatz is indeed minor.
In the following, we consider microlensing of the wormhole. We will assume that $\beta >> \alpha$ so that we are considering the weak-lensing regime. The energy density of wormhole is

$$\rho = \frac{1}{8\pi G}[\frac{1-n}{r_0^2}(\frac{r_0}{r})^{n+2}], \tag{49}$$

The two-dimensional enclosed mass for an infinite spherical density is obtained as

$$M_{2D} = \frac{1}{4G}\pi^{\frac{1}{2}}[(1-n)r_0]\frac{\Gamma(\frac{n+1}{2})}{(1-n)\Gamma(\frac{n+2}{2})}(\frac{\xi}{r_0})^{1-n} \tag{50}$$

for $n = \frac{1}{2}$ and $r_0 = 1$ we have

$$M_{2D} = \frac{1}{G}\pi^{\frac{1}{2}}\frac{\Gamma(\frac{3}{4})}{\Gamma(\frac{1}{4})}\xi^{\frac{1}{2}} \tag{51}$$

This is the mass enclosed by the cylinder interior to ξ and is obtained by integrating the projected surface mass density Σ over the area of the circle with radius ξ. In a weak field, by using of Eq. 44 for deflection angle and Eq. 19, Einstein radius will be obtained

$$R_E = (\frac{D_L D_{LS}\theta_\alpha r_0^{\frac{1}{2}}}{D_S})^{\frac{2}{3}} \tag{52}$$

where θ_α is

$$\theta_\alpha = 0.88\mu as[\frac{\Gamma(\frac{3}{4})}{\Gamma(\frac{1}{4})}](1-\frac{D_L}{D_S})(\frac{pc}{16\pi G M_\odot}) \tag{53}$$

We assume that the velocity of the wormhole is approximately equal to the rotation velocity of stars ($V_T = 220\frac{km}{s}, D_S = 8kpc$ and $D_L = 4kpc$) if it is bound to the Galaxy. If the wormhole is not bound to our Galaxy, the transverse velocity would be much higher. We assume ($V_T = 5000\frac{km}{s}, D_S = 50kpc$ and $D_L = 25kpc$) for the unbound wormhole. In Figure. 4 we show the magnification curves and display two cases for two different velocity and different impact parameters. As one can see, the light curves are similar to the light curves of the Schwarzschild point mass lenses. Also as expected as the value of the impact parameter increases, the magnification becomes weaker.

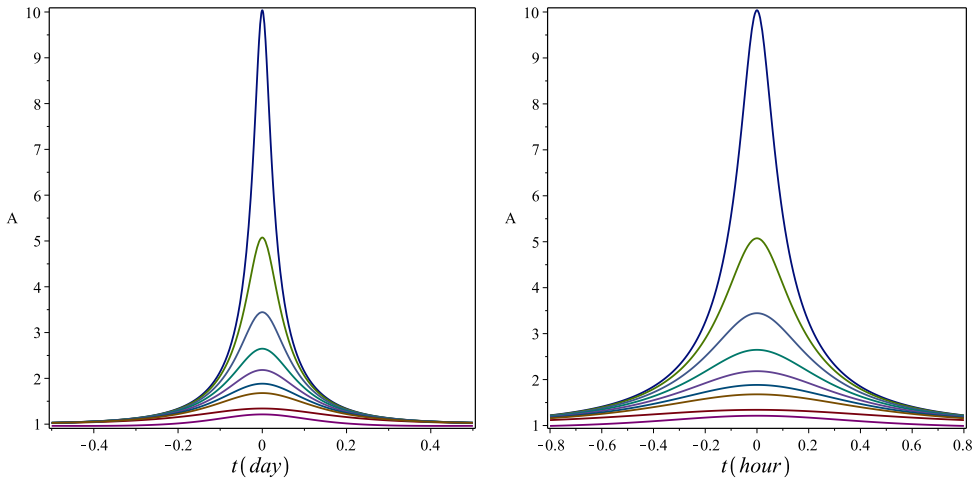

(a) (b)

Figure 4: The behaviour of amplification (A) verses time (t) for unbound wormhole at $n = \frac{1}{2}$, $r_0 = 1$, $\beta_0 = 0.1, 0.2, 0.3, 0.4, 0.5, 0.6, 0.7, 0.8, 0.9, 1$, $V_T = 220\frac{km}{s}$(left) and $V_T = 5000\frac{km}{s}$(right).

Returning to the radial equation of motion (see Figure 5), for $r > r_0$, radial acceleration is negative which means that the gravitational field of the wormhole is attractive, i.e, the free fall observer is pulled into the wormhole. Just at the throat $r = r_0$, the radial acceleration and therefore, surface gravity is zero.

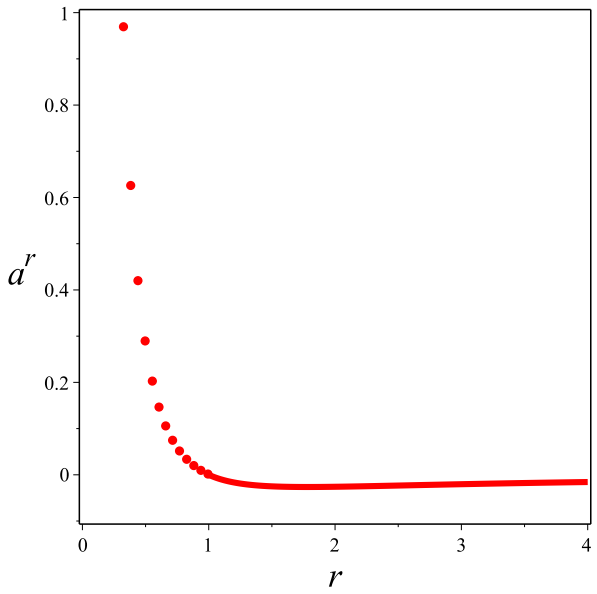

Figure 5: The behaviour of a^r for $n = \frac{1}{2}$ and $r_0 = 1$.

5 Energy conditions and exoticity parameter

As we mentioned in the introduction, the main objection against the plausibility of a wormhole solution is that the energy-momentum tensor which supports this geometry violates the weak energy condition (WEC). Violations of the pointwise energy conditions led to the averaging of the energy conditions over timelike or null geodesics. The averaged energy conditions are somewhat weaker than the pointwise energy conditions, as they permit localized violations of the energy conditions, as long as average energy conditions hold when integrated along timelike or null geodesics[4, 33]. As can be seen from Figure 6, The minimum of average energy density (dash dot blue color) is in 1, while the minimum of average $\rho + P_r$ (red color) and $\rho + P_t$(dot green color) is in 0. So the minimum violation in weak energy condition are around $n = 0$.

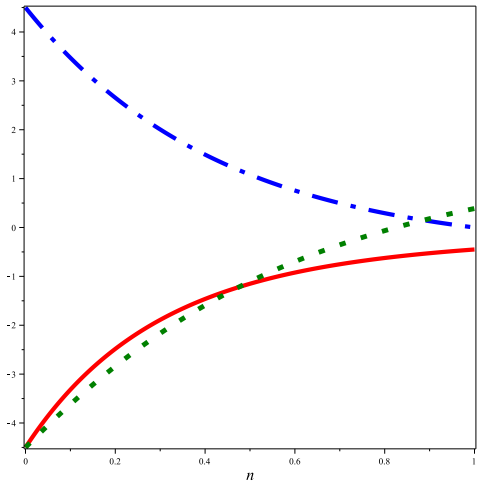

Figure 6: The behaviour of average weak energy condition in terms of n, at $r = 10r_0$.

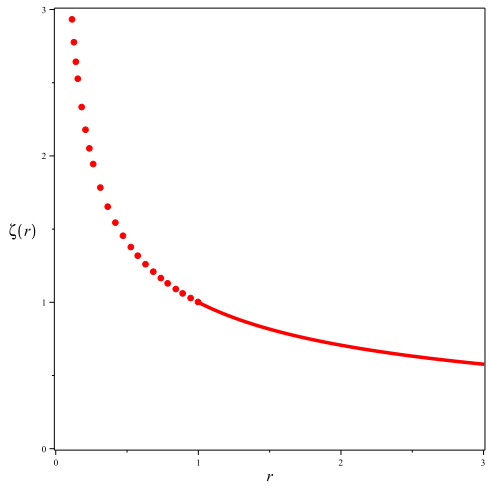

Figure 7: The behaviour of $\zeta(r)$ for $n = \frac{1}{2}$ and $r_0 = 1$.

According to Figure 7, exoticity parameter is positive over the entire wormhole space. The weak energy condition requires

$$T_{\mu\nu}u^{\mu}u^{\nu} \geq 0 \tag{54}$$

for every timelike u^{μ} which leads to

$$\rho \geq 0 \quad , \quad \rho + P_r \geq 0 \quad , \quad \rho + P_t \geq 0 \tag{55}$$

using 35, 36 and 37 we have

$$\rho \geq 0 \quad \rightarrow \quad \frac{1-n}{r_0^2}(\frac{r_0}{r})^{n+2} \geq 0 \tag{56}$$

$$\rho + P_r \geq 0 \quad \rightarrow \quad -\frac{n}{r_0^2}(\frac{r_0}{r})^{2n+2} \geq 0 \tag{57}$$

$$\rho + P_t \geq 0 \quad \rightarrow \quad \frac{(n+2)(n-1)}{2r_0^2}(\frac{r_0}{r})^{n+2} + \frac{n^2}{r_0^2}[(\frac{r_0}{r})^{2n+2} - \frac{1}{4}(\frac{r_0}{r})^{3n+2}] \geq 0 \tag{58}$$

From equation 56, we can conclude that the positive energy density condition is satisfied for $0 < n < 1$ (see Fig. 8). Furthermore, expressions 57 and 58 are negative in this range(see Fig. 9).

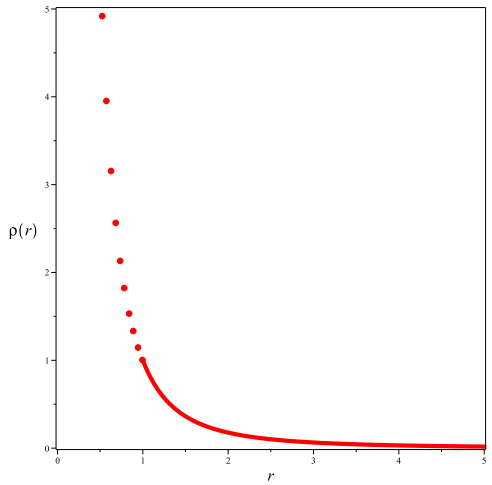

Figure 8: The behaviour of $\rho(r)$ for $r_0 = 1, n = \frac{1}{2}$.

Flare out				
ρ				
$\zeta > 0$				
$\zeta < 0$				
n	-2	-1	+1	+2

Table 1: The status of wormhole conditions versus the key parameter n. Shaded areas correspond to the violation of each condition.

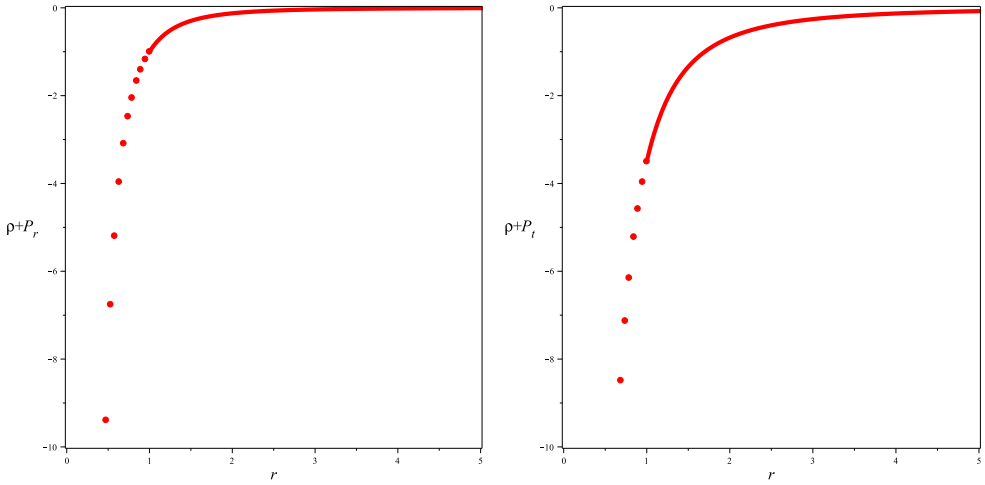

(a) (b)

Figure 9: The behavior of $\rho(r) + P_r(r)$(left) and $\rho(r) + P_t(r)$(right) for $r_0 = 1, n = \frac{1}{2}$.

6 Conclusion

In this paper, we introduced a new wormhole geometry with a multi-polytropic source. With the help of Wormhole conditions (Flare out, asymptotically flatness, positive mass), parameters were fixed ($0 < n < 1$). Full lensing (which includes both weak and strong lensing) were calculated. It was shown that the behavior of this object is very similar to the lensing behavior of a black hole, also light curves of microlensing of the positive mass (but violated energy condition) extended lens is similar to the point source object. The weak energy condition was written for the wormhole metric. Also, we learned that within the multi-polytropic EoS, static wormholes can respect the positive energy density condition all over space. By plotting $\rho + P_r$ and $\rho + P_t$ versus r, we found that these quantities are negative everywhere, thus violating the (WEC).

References

[1] L. Flamm, Physikalische Zeitschrift. **17**, 448 (1916).

[2] A. Einstein and N. Rosen, Phys. Rev. **73**, 48 (1935).

[3] A. J. Wheeler, Phys. Rev. **511**, 97 (1955).

[4] M. S. Morris and K. S. Thorne, Am. J. Phys. **395**, 56 (1988).

[5] P.K.F. Kuhfittig, Sch. Res. Exch. 296158 (2008).

[6] S. N. Sajadi and N. Riazi, Prog. Theor. Phys. **126**, 753 (2011).

[7] M. R. Mehdizadeh, M. K. Zangeneh and F. S. N. Lobo, Phys. Rev. **D 91**, 084004 (2015).

[8] H. Saiedi, Mod. Phys. Lett. **A 27**, 1250220 (2012).

[9] P. Kanti, B. Kleihaus and J. Kunz, Phys. Rev. Lett. **107**, 271101 (2011).

[10] H. Maeda and M. Nozawa, Phys. Rev. **D 78**, 024005 (2008).

[11] J. Matulich and R. Troncoso, JHEP, **1110**, 118 (2011).

[12] S. H. Mazharimousavi, M. Halilsoy and Z. Amirabi, Phys. Rev. **D81**, 104002 (2010).

[13] M. H. Dehghani and M. R. Mehdizadeh, Phys. Rev. **D 85**, 024024 (2012).

[14] J. G. Cramer, R. L. Forward, M. S. Morris, M. Visser, G. Benford, G. A .Landis, Phys. Rev. **D 51**, 3317 (1995).

[15] D. F. Torres, G. E. Romero, L. A. Anchordoqui, Phys. Rev. **D 58**, 123001 (1998).

[16] M. Safonova, F. T. Diego, G. E. Romero, Phys. Rev. **D 65**, 023001 (2001).

[17] M. B. Bogdanov, A. M. Cherepashchuk, Astrophys. Space Sci. **317**, 181 (2008).

[18] A, L, Erickcek, N, M, Law. Astrophys. J, **729**, 49 (2011).

[19] V. Bozza, Phys. Rev. **D 66**, 103001 (2002).

[20] K.S. Virbhadra, G.F.R. Ellis, Phys. Rev. **D 62**, 084003 (2000).

[21] L. A. Anchordoqui, G. E. Romero, D. F. Torres, I. Andruchow, Mod. Phys. Lett. **A 14**, 791 (1999).

[22] G. E. Romero, D. F. Torres, L. A. Anchordoqui, I. Adruchow, B. Link, Monthly Notices Royal Astron. Soc. **308**, 799 (1999).

[23] S. Chandrasekhar, An Introduction to the Study of Stellar Structure (University of Chicago, Chicago, 1939).

[24] S. L. Shapiro and S. A. Teukolsky, Black Holes, White Dwarfs and Neutron Stars (John Wiley and Sons, New York, 1983).

[25] R. Kippenhahn and A. Weigert, Stellar Structure and Evolution (Springer Verlag, Berlin, 1990).

[26] A. Kovetz, Astrophys. J. **154**, 999 (1968).

[27] R. Tooper, Astrophys. J. **140**, 434 (1964).

[28] L. Herrera, W. Barreto, Phys. Rev. **D 88**, 084022 (2013).

[29] C. F. McKee, J. H. Holliman, Astrophys. J, **522**, 313 (1999).

[30] M. Jamil, P. K. F. Kuhfittig, F. Rahaman, Sk. A Rakib, Eur. Phys. J, **C 67**, 513-520 (2010).

[31] P. H. Chavanis, Eur. Phys. J. Plus, **129**, 38 (2014).

[32] O. Bertolami, J. Paramos, Phys. Rev. **D 72**, 123512 (2005).

[33] F. S. N. Lobo, Classical and Quantum Gravity Research, Nova Sci. Pub. ISBN 978-1-60456-366-5, 1-78, (2008).

[34] M. Visser, Lorentzian Wormholes (AIP Press, New York, 1996).Soc. **308**, 799 (1999).

[35] E. Ebrahimi and N. Riazi, Phys. Rev. **D 81**, 024036 (2010).

[36] Bin-Nun, Amitai Yisrael, Publicly Accessible Penn Dissertations. Paper 252, (2010).

[37] J. M. Tejeiro, A. Larranaga, Rom. Journ. Phys, **57**, 736-747 (2012).

[38] Kamal Kanti Nandi, Yuan-Zhong Zhang, Alexander V. Zakharov, Phys. Rev. **D 74**, 024020 (2006) .

[39] F. Abe, Ap. J, **725**, 787-793 (2010).

[40] E. Eiroa, G. E. Romero, D. F. Torres, Mod. Phys. Lett, **A 16**, 973-984 (2001).

[41] Peter K. F. Kuhfittig, Eur. Phys. **J 74**, 2818 (2014).

[42] K. S. Virbhadra and G. F. R. Ellis, J. Math. Phys. **42**, 818-838 (2001).

[43] K.K. Nandi, A.I. Filippov, F. Rahaman, S. Ray, A.A. Usmani, M. Kalam, and A. DeBenedictis, Mon. Not. Roy. Astron. Soc. **399**, 2079 (2009).

[44] G. L. Bryan, M. L. Norman, Ap, **J 495**, 80 (1998).

[45] Peter K.F. Kuhfittig, Fundamental J. Mod. Phys. **7**, 111-119 (2014).